Preliminary Design of NIF 2-D SSD

Introduction

Direct-drive operation of the National Ignition Facility (NIF) will require broadband beam smoothing to successfully implode a direct-drive inertial confinement fusion (ICF) capsule and achieve high gain.[1] The base-line system parameters for NIF beam smoothing with two-dimensional smoothing by spectral dispersion (2-D SSD) are 1-THz total bandwidth in the ultraviolet, 50 × 100-μrad laser divergence, and 2 × 1 color cycle.

Broadband-beam-smoothing techniques critical to high-performance direct-drive implosions have been demonstrated successfully on OMEGA.[2] Two different configurations of a 2-D SSD system have been employed to improve irradiation uniformity. One mode producing a 1-THz bandwidth in the ultraviolet with approximately one color cycle in each SSD dimension dramatically improved direct-drive target performance, while another mode operating at only 0.35-THz bandwidth but with three color cycles in one direction also exhibited substantial benefits.[3] Both broadband 2-D SSD systems depended on a high-frequency, bulk phase modulator to realize these beam-smoothing improvements.[4]

As a partner in the National Inertial Confinement Fusion (ICF) Program, LLE has taken a lead role in defining direct-drive requirements for NIF and preparing a preliminary 2-D SSD system design to meet the beam-smoothing requirements. A prototype NIF 2-D SSD preamplifier module (PAM**)** will be built and tested in the Laser Development Laboratory at LLE to demonstrate satisfactory performance before transferring it to LLNL, where it will be integrated into the Preamplifier Module Laboratory. This article provides a summary of this design, including discussions of NIF features that constrain the design and direct-drive requirements.

NIF Features Influencing the 2-D SSD Design

Two aspects of NIF's direct-drive operation dictate a different 2-D SSD system architecture than was demonstrated on OMEGA:

- the longer pulses required to drive ignition-scale targets, which increases the threat of pinhole closure in the laser system's spatial filters, and
- the extremely compact space limitations of the 48 independent PAM's.

1. Pinhole Closure

Pinhole closure occurs when plasma created at the edge of a spatial-filter pinhole expands into the region of the pinhole where the laser pulse is transmitted, as shown in Fig. 85.41(a). Pinhole closure is particularly troublesome for 2-D SSD operation since the large divergence of a beam smoothed with this technique fills a large fraction of the pinhole. Plasma interactions with the beam reduce the total 2-D SSD bandwidth propagated to the target and can even distort the beam profile or retroreflect the beam, which can cause laser damage. OMEGA pulse lengths are limited to less than 3.8 ns by these pinhole closure concerns.

Pulse lengths of the order of 10 ns are required for direct-drive NIF ignition capsules.[5] This is long enough to cause significant pinhole closure, particularly for the large, 100 × 50-μrad divergence required for high-gain, direct-drive target performance. Fortunately, it is anticipated that this large 2-DSSD diver gence will be required only during the "foot" portion of the drive, when laser imprinting occurs. One solution to this problem is dynamically reducing the laser divergence after sufficient smoothing is applied, but before pinhole closure interferes with the beam. Detailed laser imprint experiments on OMEGA and early laser experiments on the NIF using a subset of beams outfitted with 2-D SSD will be required to establish the dynamic profile of this approach. Additional experiments will be performed to establish the lower limit of SSD bandwidth required late in the drive pulse to mitigate adverse laser–plasma interactions.

Since laser divergence is directly related to the product of grating dispersion and SSD bandwidth, dynamic SSD band-

width reduction can be implemented to achieve the desired reduction. Two different approaches are available to realize dynamic bandwidth reduction. First, the microwave signal applied to a phase modulator producing the SSD bandwidth can be reduced or turned off. This approach, shown in Fig. 85.42(a), requires fast microwave switches and an electro-optic modulator with sufficient bandwidth. Highly resonant phase modulator designs like the bulk modulators used in OMEGA are unsuitable for this application, but traveling-wave integrated optic devices are commercially available.[6] Fast microwave devices with switching times of approximately 2 ns, which may be satisfactory for this application, are also available.[7]

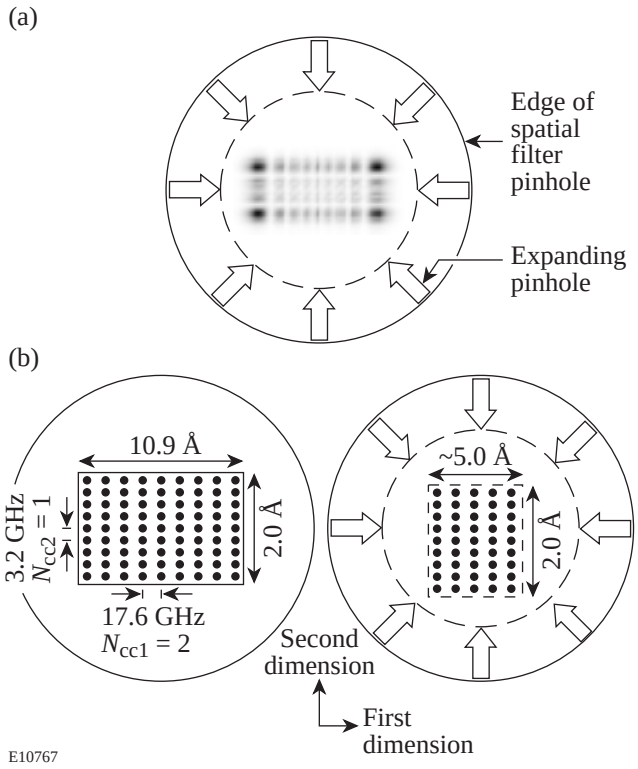

Figure 85.41
(a) Laser energy deposited at the edge of a spatial-filter pinhole creates a plasma that expands into the center of the pinhole. Pinhole closure is particularly troublesome with 2-D SSD beams since a large fraction of the pinhole is filled and the far-field energy distribution for phase-modulated 2-D SSD beams is corner-peaked. Interactions of the pinhole plasma with the SSD sidebands also convert phase modulation into amplitude modulation. (b) Dynamic bandwidth reduction can minimize the impact of pinhole closure by reducing the beam divergence before the pinhole closure affects the beam. A schematic representation of dynamic bandwidth reduction shows how full beam smoothing will be achieved during the foot of the pulse with reduced bandwidth later in the pulse.

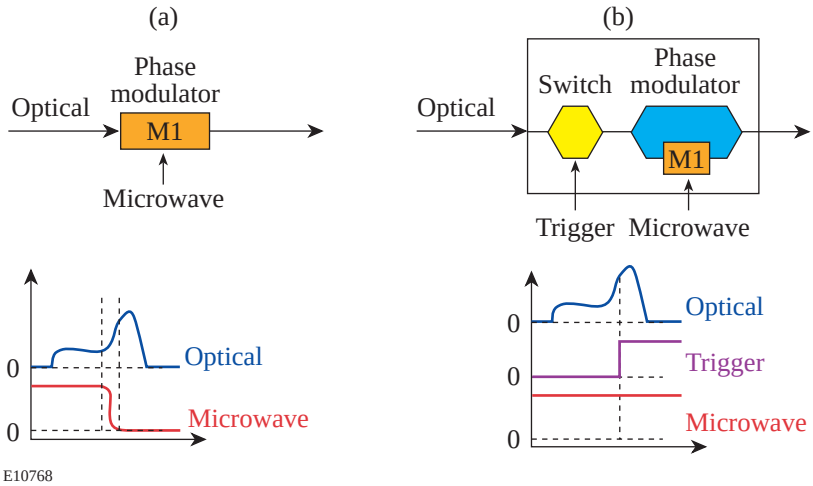

Figure 85.42
Dynamic bandwidth reduction can be implemented either electrically or optically. (a) Switching the microwave power delivered to an integrated-optic phase modulator poses the simplest approach since fast microwave switches are available, but switching times are limited to approximately a nanosecond. (b) Optical methods might also be applied to dynamically reduce SSD bandwidth during the pulse. One approach would direct the initial portion of the pulse through a phase modulator and then bypass the modulator during the latter portion.

An alternate approach to realizing dynamic bandwidth reduction for direct-drive NIF involves "optically splicing" two pulses with different SSD bandwidths, as shown in Fig. 85.42(b). This scheme produces the drive pulse in two separate sections that are combined to form the desired pulse shape and SSD bandwidth profile.

"Optical pulse splicing" offers a potential for extremely fast bandwidth reductions limited only by optical switching times of the order of ~40 ps, plus a straightforward approach for doubling the pulse-shaping contrast. Two separate front-end laser systems would be required in the Master Oscillator Room (MOR) to realize these improvements; some development would also be required. This approach is compatible with implementing ultrafast picket-fence pulses in the foot of the drive pulse, which is currently being evaluated to improve frequency-conversion efficiency and power balance.[8]

Microwave switching was selected for the base-line dynamic bandwidth reduction system since it utilizes existing technology. Preliminary design of this system has started and will be demonstrated in the NIF 2-D SSD PAM test-bed. Either approach is consistent with the all-fiber-optic front-end architecture currently implemented on the NIF.

2. Preamplifier Module (PAM) Space Constraints

A significant constraint on the NIF 2-D SSD design is the tight space limit imposed by the PAM design. A modular 2-D SSD design will be pursued so that 2-D SSD beam smoothing can be retrofitted into the first NIF PAM's built for indirect drive that will not include this feature. The PAM design integrates a high-gain, Nd:glass regenerative amplifier, beam shaping, and a four-pass amplifier on a single optical breadboard assembly that composes a line replaceable unit (LRU). In comparison, these same functions are realized in OMEGA on two large optical tables. A 2-D SSD module must fit within the PAM LRU envelope for NIF, whereas for OMEGA this functionality occupies another 4-ft × 14-ft optical table that is larger than the entire PAM assembly, shown in Fig. 85.43(a).

One side of the PAM includes the regenerative amplifier and beam-shaping module (BSM), as shown in Fig. 85.43(b). A shaped pulse launched into free space from an optical fiber is mode matched to the regenerative amplifier. This *Q*-switched cavity amplifies the pulse to approximately 20 mJ. After cavity dumping the pulse, two isolation Pockels cells provide high prepulse contrast. The beam-shaping module expands the pulse and reshapes the Gaussian beam into the square profile required to compensate the NIF gain with a serrated aperture and transmission masks. The BSM output pulse is approximately 2 mJ and is directed to the four-pass amplifier on the other side of the PAM assembly.

The four-pass amplifier side of the PAM, depicted in Fig. 85.43(c), produces up to a 17-J output pulse required to inject four separate NIF main amplifiers. A location is provided inside the four-pass amplifier for the 1-D SSD grating required for indirect drive. This side of the PAM is extremely compact.

NIF's 2-D SSD Preliminary Design

Figure 85.44 schematically highlights portions of the NIF architecture relevant to 2-D SSD. The seed pulse for all 192 NIF beams originates in the Master Oscillator Room (MOR) from a continuous-wave, single-frequency, fiber laser that is subsequently sliced into pulses and amplified. Frequency modulation is applied to the pulse by an integrated-optic phase modulator (M1). This device is actually three separate phase modulators integrated into a single package. One modulator applies a small amount of bandwidth (~0.5 Å) at a modulation frequency of ~3 GHz, which is required to suppress transverse stimulated Brillouin scattering (SBS) in the large NIF optics. The remaining two modulators are used to apply SSD bandwidth for beam smoothing. After bandwidth is applied in M1, the seed pulse is split and amplified into 48 channels, which supply each of the PAM's. All pulses with FM bandwidth are transported by polarizing (PZ) fiber to minimize FM-to-AM conversion caused by polarization mixing at fiber connectors. An arbitrary waveform generator (AWG) shapes the input pulse and provides fine timing for each PAM.

In addition to the amplification and beam shaping in the PAM, a 2-D SSD module will be added that can be bypassed during non-direct-drive NIF operation to avoid the additional system complexity and insertion loss when it is not required. Most of the 2-D SSD module will be located on the regenerative amplifier side of the PAM, including

- a "rolled" reflection grating (G2/G3),
- a bulk phase modulator (M2),
- spatial filters and telescopes required to control beam size and image relay the beam from the serrated aperture (RP_0) into the four-pass amplifier, and
- Faraday isolation stages used to double pass both the G2/G3 grating and bulk modulator.

It is significant to note that a precompensation grating (G1) for the first SSD direction is not possible with this design since the integrated-optic phase modulator (M1) is a single transverse mode device. As a result, the pulse shape is distorted by the G2/G3 grating, which is a reflection grating operated at the Littrow angle. This grating also precompensates the pulse before the second dimension of SSD bandwidth is applied by the bulk modulator (M2) and dispersed by the G4 grating. Both the first SSD dimension dispersion (G2) and second SSD dimension precompensation (G3) grating functions are accomplished with a single grating by "rolling" the grating about its input (Littrow) axis, as shown in Fig. 85.45.

The NIF 2-D SSD bulk modulator will be based on an existing OMEGA design.[9] The M2 bandwidth is dispersed in an orthogonal direction by a second 2-D SSD grating (G4)

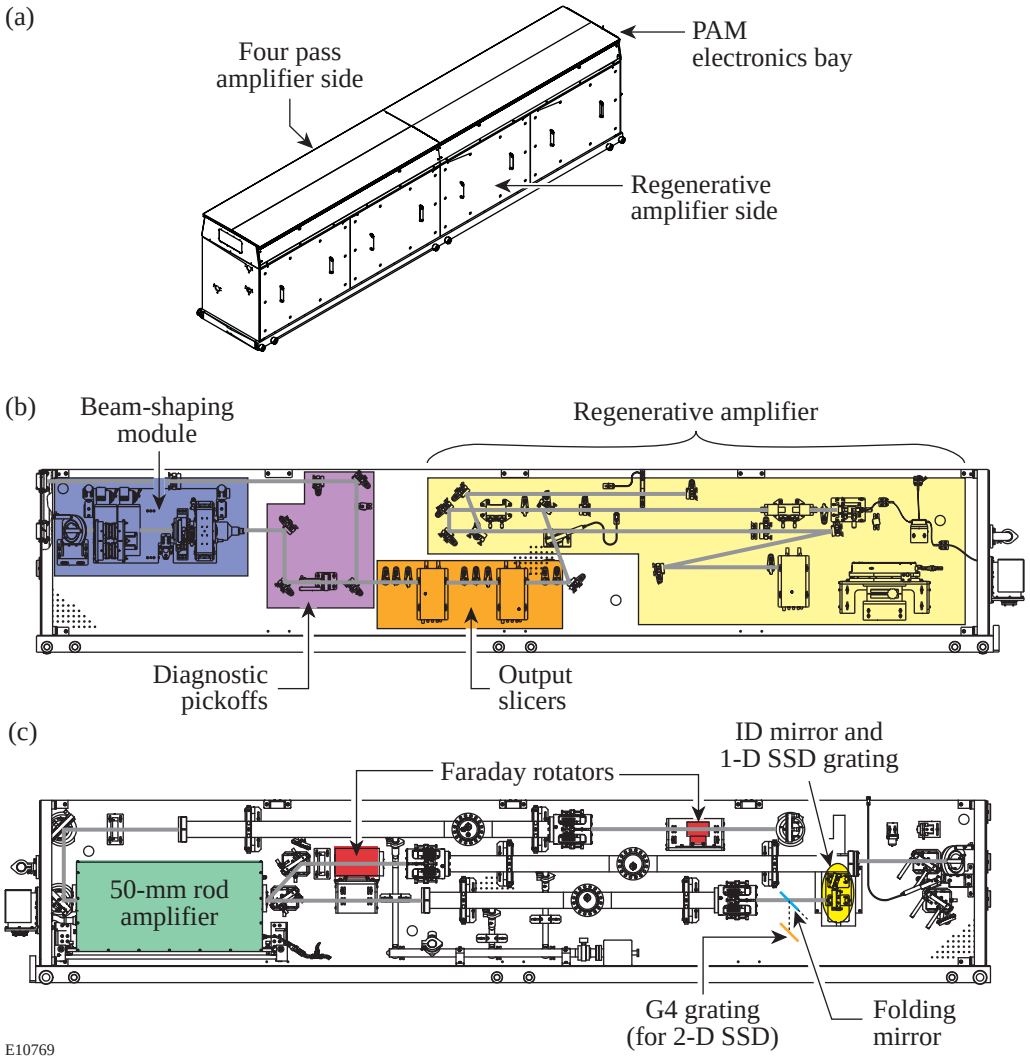

Figure 85.43
The NIF preamplifier module (PAM) poses severe space constraints on implementing 2-D SSD beam smoothing. (a) The PAM is a self-contained "line replaceable unit" that includes a regenerative amplifier (regen) and beam-shaping module (BSM) on one side of a vertically mounted optical breadboard and a four-pass amplifier on the other side. (b) The regen and BSM are highly engineered systems that ideally would require no changes when implementing a 2-D SSD module in the PAM. (c) The four-pass amplifier side is extremely compact but will require only the addition of another grating to disperse the bandwidth produced by the bulk phase modulator.

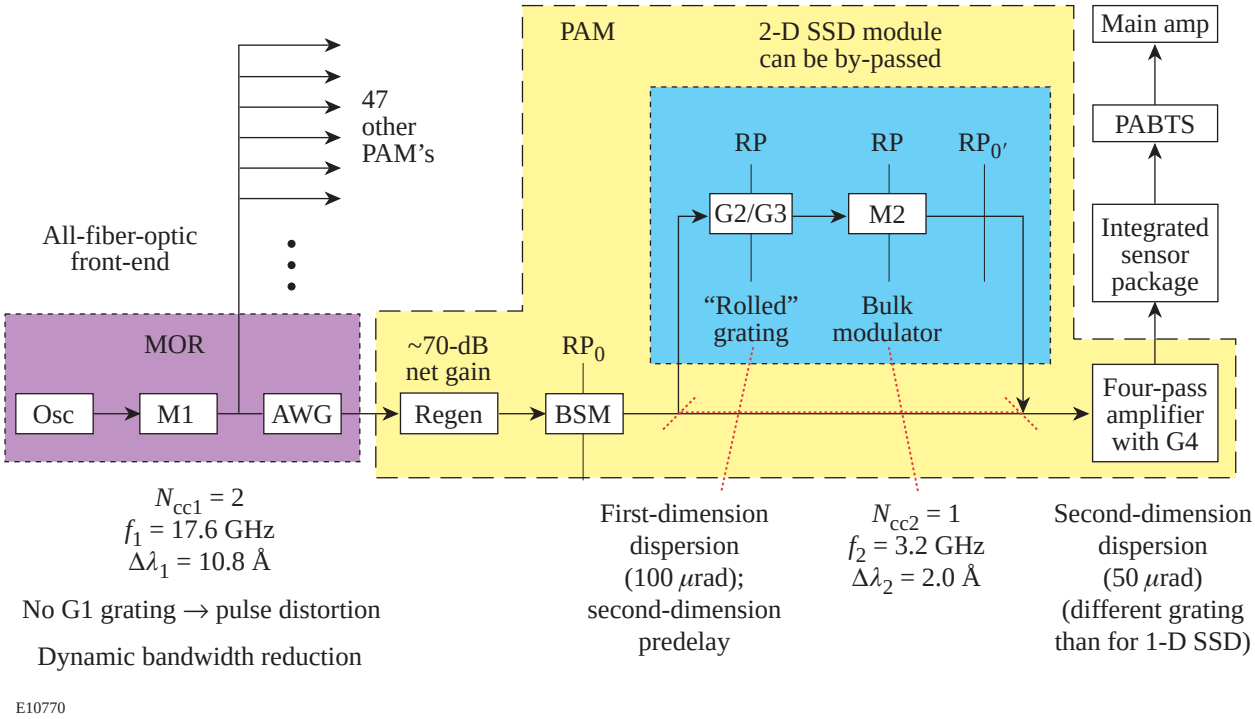

Figure 85.44
NIF architecture is significantly different from OMEGA. An all-fiber-optic front-end generates and distributes shaped pulses to 48 PAM's. The first 2-D SSD modulator (M1) is an integrated-optic phase modulator located in the Master Oscillator Room (MOR), but separate bulk modulators are required in each PAM. The BSM magnifies and spatially shapes the regen output pulse. The 2-D SSD module must be located after the BSM, where the pulse energy is lower, to avoid damaging the bulk modulator and to maximize the beam size.

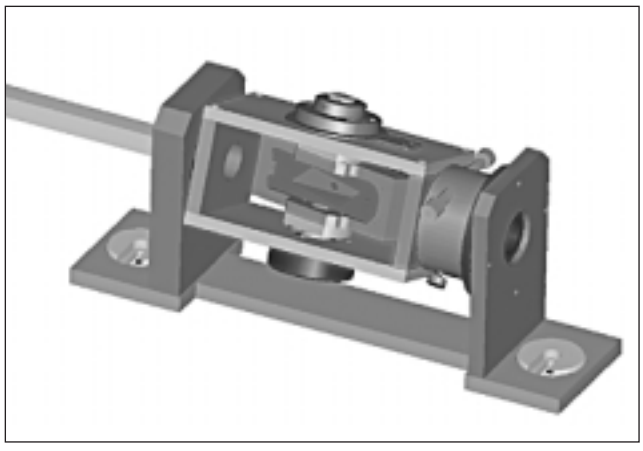

Figure 85.45
A "rolled" reflection grating performs two separate 2-D SSD grating functions by taking advantage of the vector nature of grating dispersion. It disperses the bandwidth produced by the integrated-optic modulator, and it precompensates the distortion introduced by the grating that disperses the bandwidth produced by the bulk modulator. These grating functions are identified using the same OMEGA convention as G2/G3 and G4, respectively.

located in the four-pass amplifier, as shown in Fig. 85.43(c). The G4 grating required for 2-D SSD is different from the 1-D SSD grating currently implemented for indirect-drive operation. All SSD gratings are located at image-relay planes of the serrated aperture (RP_0) in the BSM, which is image relayed throughout the laser system. After the PAM, the alignment, energy, and pulse shape of the PAM output beam are diagnosed by the integrated sensor package (ISP) and transported to the NIF's main amplifiers by the preamplifier beam transport system (PABTS).

Description of the NIF PAM Operation with a 2-D SSD Module

Figure 85.46 represents the base-line layout of the regenerative amplifier side of the PAM in which a 2-D SSD module can be realized. A key aspect of this design is that the regenerative amplifier and beam-shaping module are unchanged, and only minor changes to the existing isolation stage and diagnostic pickoffs are required to provide adequate space for the 2-D SSD module. The isolation Pockels cells are reoriented and more compactly arranged to free up space for the G2/G3 grating telescope at the bottom of the PAM, as well as in the main section of the 2-D SSD module located adjacent to the BSM. Additionally, the centering glass (RC1), diagnostic wedge (RS1), and folding mirror assemblies are reconfigured to further increase the space envelope available for the 2-D SSD module.

The output direction from the BSM will be remotely selectable by a new BM1/SM1 mirror stage. A single mirror is used to select whether the beam proceeds directly to the four-pass amplifier (BM1) for non-direct-drive operation or is diverted into the 2-D SSD module (SM1) for direct-drive operation. Figure 85.47 shows both of these configurations. This scheme provides a 2-D SSD bypass that will not affect 1-D SSD performance for indirect-drive operations, plus it does not require relocating the BSM. Operation of the 2-D SSD module is described below.

The 30-mm-square beam produced by the BSM is down-collimated by a 4× input spatial filter to a 7.5-mm-square beam (~10.6-mm diagonal) to fit through a 15-mm-clear-aperture Faraday rotator (SFR1). The spatial-filter pinhole removes high-spatial-frequency components introduced by the serrated aperture and beam-shaping masks in the BSM before the beam is imaged into the bulk phase modulator. The pinhole assembly will include the ability to remotely select its position to either "IN" or "OUT" to facilitate alignment operations. The first Faraday isolation stage extracts the pulse from the double-pass grating section of the 2-D SSD module.

The 2.25× grating telescope magnifies the beam to the correct size to achieve two SSD color cycles for the integrated-optic modulator (M1) operating at 17.6 GHz, plus to pre-compensate a single color cycle for the bulk modulator (M2)

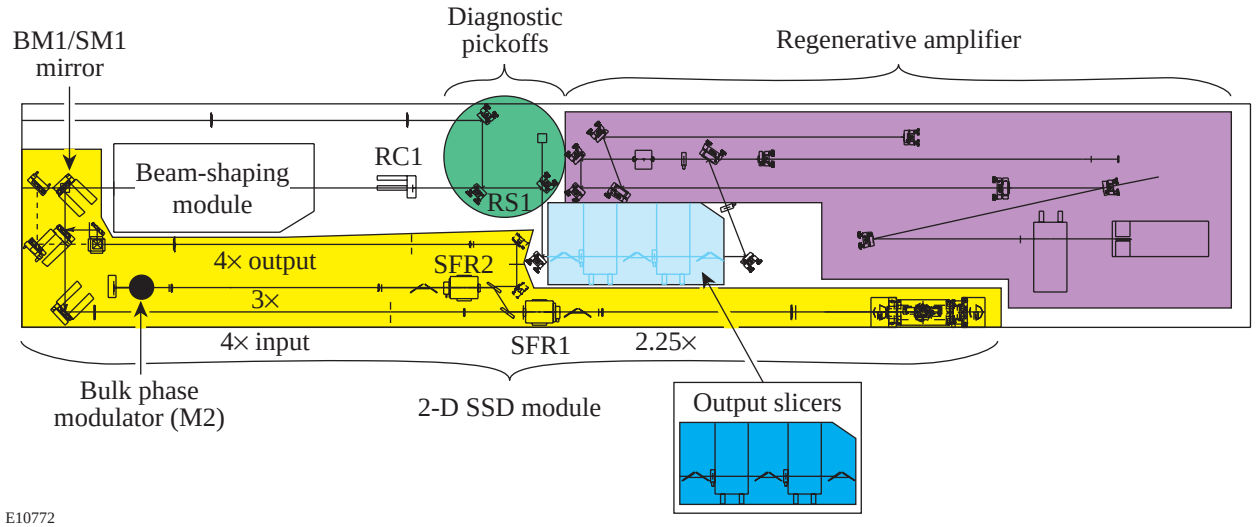

Figure 85.46
The regen side of the PAM will require minor modifications to accommodate a 2-D SSD module, but the regen and BSM will not need to be changed. The 2-D SSD module includes an input spatial filter, two Faraday isolation stages for the double-pass grating and modulator legs that include image relays, and an output spatial filter. A rotating mirror assembly (shown in Fig. 85.47) selects either indirect-drive or direct-drive PAM operation.

operating at 3.2 GHz. This image relay is sandwiched between two quarter-wave plates and preceded by polarizers to provide first-order ghost suppression in the double-pass section. Ultra-low-reflectivity antireflection (AR) coatings ($R \leq 0.05\%$) are also specified for the lenses to minimize ghost reflections since first-order ghosts will produce undesirable prepulses.

The G2/G3 reflection grating disperses the M1 bandwidth in each of two orthogonal components. The component normal to the plane of the PAM breadboard corresponds to the 100-μrad SSD divergence direction, while the in-the-plane component is matched but opposite to the dispersion produced by the G4 grating that produces the 50-μrad SSD divergence.

After the pulse is extracted from the double-pass grating section, it is injected into the double-pass bulk modulator section by a reflection off the input polarizer, in the second Faraday isolation stage. A 3× bulk modulator telescope demagnifies the beam to a 3-mm-square beam that fits the 5-mm × 6-mm-aperture bulk modulator. Like the grating telescope, first-order ghost suppression is achieved with quarter-wave plates, double polarizers, and ultra-low-reflectivity AR-coated lenses.

The bulk modulator (M2) employs a $LiNbO_3$ crystal with 1°-wedged, AR-coated input surface. A retroreflecting mirror positioned behind M2 serves to double pass the modulator crystal. The return path length is carefully set to phase match the microwave and optical fields in the modulator during the second pass.

The beam height within most of the 2-D SSD module is 105 mm. An image rotation periscope lowers the 2-D SSD beam height to 45 mm. This beam height is required to reinject the beam back into the path toward the four-pass amplifier. The beam is reinjected using a mirror located between the SM1 mirror and the breadboard hole, as shown in Fig. 85.47. The image rotation periscope also rotates the beam 90° to compensate for an additional 90° rotation introduced when the beam is passed through the PAM breadboard into the four-pass amplifier.

Both the BSM and the 2-D SSD module output beams are delivered through leaky mirrors to the ISP for alignment operations and can be individually selected by shutters (not shown).

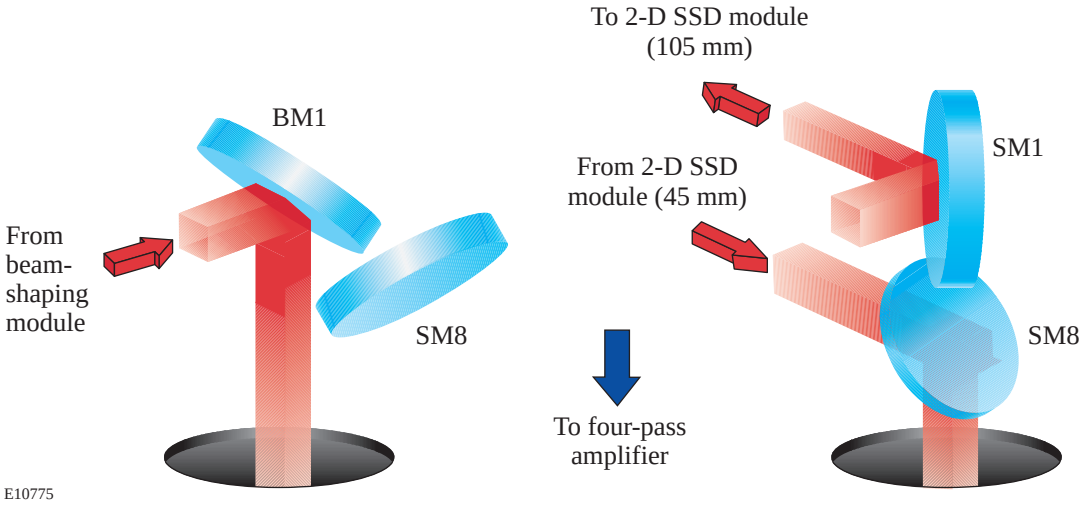

Figure 85.47
PAM operation in either the indirect-drive (2-D SSD bypassed) or direct-drive modes will be remotely selectable. A single mirror assembly rotating around the beam-shaping module's output axis will be used to reflect the beam either directly to the four-pass amplifier side of the PAM or into the 2-D SSD module. This mirror is designated BM1/SM1 and functions as a remotely operable centering mirror to support alignment in either mode. A second mirror in this rotating assembly (SM8) swings under the BM1/SM1 mirror to reflect the 2-D SSD module output beam that is returned at a 45-mm beam height. Remotely operable mirror SM7, shown in Fig. 85.46, provides the centering function during 2-D SSD operation since mirror SM8 must be stationary.

Conclusion

Direct-drive NIF operation will require a two-color-cycle, 1-THz 2-D SSD system to achieve beam smoothing required for ignition with high gain. A preliminary 2-D SSD design has been outlined in this article that is compatible with the NIF architecture and the existing PAM design. Detailed design is underway, and a prototype 2-D SSD module will be demonstrated at LLE before transferring it to LLNL for integration testing.

ACKNOWLEDGMENT

This work was supported by the U.S. Department of Energy Office of Inertial Confinement Fusion under Cooperative Agreement No. DE-FC03-92SF19460, the University of Rochester, and the New York State Energy Research and Development Authority. The support of DOE does not constitute an endorsement by DOE of the views expressed in this article.

REFERENCES

1. Laboratory for Laser Energetics LLE Review **84**, 181, NTIS document No. DOE/SF/19460-371 (2000). Copies may be obtained from the National Technical Information Service, Springfield, VA 22161.

2. Laboratory for Laser Energetics LLE Review **80**, 197, NTIS document No. DOE/SF/19460-321 (1999). Copies may be obtained from the National Technical Information Service, Springfield, VA 22161.

3. D. D. Meyerhofer, J. A. Delettrez, R. Epstein, V. Yu. Glebov, R. L. Keck, R. L. McCrory, P. W. McKenty, F. J. Marshall, P. B. Radha, S. P. Regan, W. Seka, S. Skupsky, V. A. Smalyuk, J. M. Soures, C. Stoeckl, R. P. J. Town, B. Yaakobi, R. D. Petrasso, J. A. Frenje, D. G. Hicks, F. H. Séguin, C. K. Li, S. Haan, S. P. Hatchett, N. Izumi, R. Lerche, T. C. Sangster, and T. W. Phillips, "Core Density and Temperature Conditions and Fuel–Pusher Mix in Direct-Drive ICF Implosions," to be published in Physics of Plasmas; T. R. Boehly, V. N. Goncharov, O. Gotchev, J. P. Knauer, D. D. Meyerhofer, D. Oron, S. P. Regan, Y. Srebro, W. Seka, D. Shvarts, S. Skupsky, and V. A. Smalyuk, "Optical and Plasma Smoothing of Laser Imprinting in Targets Driven by Lasers with SSD Bandwidths up to 1 THz," *ibid.*; Laboratory for Laser Energetics LLE Review **84**, 173, NTIS document No. DOE/SF/19460-371 (2000). Copies may be obtained from the National Technical Information Service, Springfield, VA 22161.

4. Laboratory for Laser Energetics LLE Review **78**, 53, NTIS document No. DOE/SF/19460-295 (1999). Copies may be obtained from the National Technical Information Service, Springfield, VA 22161.

5. C. P. Verdon, Bull. Am. Phys. Soc. **38**, 2010 (1993); Laboratory for Laser Energetics LLE Review **79**, 121, NTIS document No. DOE/SF/19460-317 (1999). Copies may be obtained from the National Technical Information Service, Springfield, VA 22161.

6. Alenia Marconi Systems, 00131 Roma, Italy (http://www.crisel-instruments.it/alenia/html/index01.htm) (2000).

7. MITEQ, Inc., Hauppauge, NY 11788 (http://www.miteq.com) (1999); M/A-COM, Inc., Lowell, MA 01853 (http://www.macom.com) (2000).

8. J. E. Rothenberg, Appl. Opt. **39**, 6931 (2000); J. A. Marozas and J. D. Zuegel, Bull. Am. Phys. Soc. **45**, 327 (2000).

9. Laboratory for Laser Energetics LLE Review **68**, 192, NTIS document No. DOE/SF/19460-139 (1996). Copies may be obtained from the National Technical Information Service, Springfield, VA 22161.